

Cite this: *Soft Matter*, 2011, **7**, 2321

www.rsc.org/softmatter

COMMUNICATION

Deformation induced pattern transformation in a soft granular crystal

F. Göncü,^{cd} S. Willshaw,^b J. Shim,^a J. Cusack,^b S. Luding,^c T. Mullin^b and K. Bertoldi^{*a}

Received 2nd December 2010, Accepted 28th January 2011

DOI: 10.1039/c0sm01408g

We report the results of an experimental and numerical investigation into a novel pattern transformation induced in a regular array of particles with contrasting dimensions and softness. The results indicate new directions for the creation of soft solids with tunable acoustic and optical properties.

It has been realized in recent years that buckling instabilities in elastomeric periodic foams can give rise to counterintuitive pattern switching phenomena^{1,2} with potential for phononic^{3,4} and photonic⁵ tunability. An interesting question to ask is whether this richness in behaviour will exist in a broader class of problems.

Ordered arrays of particles are excellent candidates for components of future acoustic, optical and electronic devices and important advances have been reported in the fabrication of such structures at the micro- and nano-scale.^{6,7} Here, we consider the discrete problem of a highly regular array of particles arranged on a two dimensional periodic lattice *i.e.* a granular crystal (Fig. 1a) and we explore its behaviour under uniaxial compression.

We report the results of an experimental and numerical study of a pattern transformation in a regular array of millimetre-scale cylindrical particles with contrasting dimensions and softness. Under uniaxial compression the system undergoes a rearrangement which leads to a new periodic pattern (Fig. 1b). The details of the transformation process depend on the size ratio of the constituent particles but the final state after compression is robust. At small ratios it is homogeneous and approximately reversible *i.e.* the initial geometry is almost recovered after unloading. In contrast, when the size ratio is increased the same final pattern is reached but now involves the sudden rearrangement of the particles *via* the formation of a shear band. The robustness of the experimental results and the scalability of the numerical work suggests a way of creating novel soft solids with interesting acoustic and optical properties.

The building blocks of the crystal are two types of cylindrical particles with different dimensions and mechanical properties. Soft particles, which are larger in diameter, are cast from the addition-

curing silicone rubber “Sil AD Translucent” (*Feguramed GmbH*, with Young modulus $E = 360$ kPa) and the “hard” cylinders are machined from a PTFE (Young modulus $E = 1$ GPa) rod. The average height of soft and hard particles were measured 9 ± 0.5 mm and 9 ± 0.02 mm, respectively.

The initial configuration consisted of hard and soft particles placed on two embedded square lattices. Each experimental configuration was constructed carefully by hand and repeatability checks were performed on stress/strain datasets. The distances between the particles were such that they touched but were not compressed (see Fig. 1c). Focus in the experiments was on investigations of two crystals formed from particles with size ratios $\chi = r/R$ where r and R are the radii of hard and soft particles, respectively. The first one with $\chi = 0.53$ consists of a 7 by 9 array of 2.7 mm radius hard particles embedded in a 8 by 10 array of 5.1 mm radius soft particles. The second one with size ratio $\chi = 0.61$ is a 9 by 9 array of 3.1 mm radius hard particles embedded in a 10 by 10 array of 5.1 mm radius soft particles. The crystals were assembled manually into a PMMA housing with dimensions which preserved the horizontal and vertical spacings between the particles.

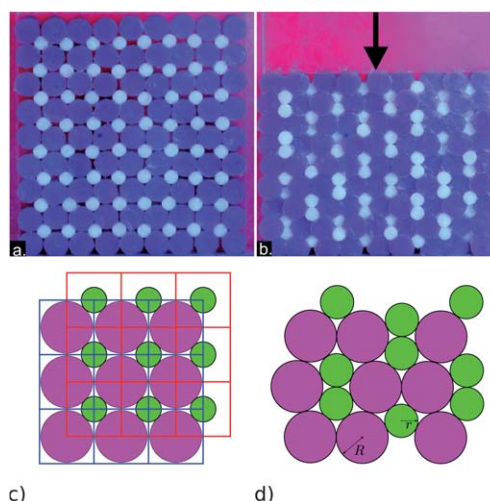


Fig. 1 (a) Initial configuration of the 2D granular crystal. (b) Deformed configuration of the crystal at 30% uniaxial compression. (c) The initial structure of the crystal consists of two embedded square lattices for small and large particles. (d) The final pattern consists of a vertically aligned pair of small particles surrounded by 6 large ones.

^aSchool of Engineering and Applied Sciences, Harvard University, Cambridge, Massachusetts, 02138, USA. E-mail: bertoldi@seas.harvard.edu; Tel: +01617 496 3084

^bManchester Centre for Nonlinear Dynamics, University of Manchester, Oxford Road, Manchester, M13 9PL, UK

^cMultiscale Mechanics, University of Twente, PO Box 217, 7500 AE Enschede, Netherlands

^dNanostructured Materials, DelftChemTech, Delft University of Technology, Julianalaan 136, 2628 BL Delft, Netherlands

Experiments were performed using a 1 kN load cell on an “Instron 5569” machine and compression was applied to the top surface of the granular crystal at a constant speed of 1 mm s^{-1} up to a strain (ϵ) of 0.25 relative to its original height, with fixed lateral walls. Before each experiment, all cylinders were coated with Vaseline to help reduce friction. For each experiment the stress–strain data was recorded and stored for post-processing and analysis.

The commercial software package Abaqus/Explicit was used to perform the finite element (FEM) simulations. Both large–soft and small–hard particles were modelled as nearly incompressible neo-Hookean⁸ solids with Poisson ratio $\nu = 0.49$ and Young’s moduli as mentioned above. Friction between contacting particles was accounted for using a Coulomb friction model with $\mu = 0.01$. The simulations were performed under plain stress conditions using a quasi-2D mesh to reduce computational cost, and the results match the experimental data reasonably well. Note that out-of-plane displacements are observed during the experiments, making the setup closer to plain stress conditions.

In addition to FEM, a 2D soft particle Molecular Dynamics (MD) approach⁹ was used to simulate the pattern transformation due to its computational advantage. The force f between contacting particles is determined by $f(\delta) = k_1\delta + k_2\delta^\alpha$, where δ is the geometrical overlap. Numerical values of the fit parameters k_1 , k_2 and α were obtained from contact simulations performed with FEM for ranges of pairs of particles. A Coulomb type friction between particles was used with $\mu = 0.01$. In addition to normal and tangential contact forces artificial damping proportional to the particle velocity was added. It should be noted that the simplification of particle deformations by geometrical overlaps is best suited for small strains where point contacts can be assumed. Soft particle MD assumes uncoupled contacts (*i.e.* the force-overlap relationship does not depend on the number of contacts) which obviously neglects volumetric effects at large deformations. Therefore, this approach may not be appropriate beyond certain particle deformation.

The pattern transformation is captured both by FEM and MD simulations. Snapshots taken from the experiments and FEM simulations for the small size ratio crystal ($\chi = 0.53$) at intermediate (15%), maximum (25%) and zero strain after unloading are shown in Fig. 2a–f. The pattern transformation in this case occurs gradually and homogeneously over the packing. The full pattern (*i.e.* the pairing of hard particles) is complete at around 20% deformation and after unloading, the initial square lattice is approximately recovered. Reversible structural rearrangements have been also observed in localized zones of 2D foams undergoing cyclic shear.¹⁰ The stress–strain curves obtained from the experiment and the numerical simulations are shown in Fig. 2g. We attribute the stronger hysteresis in the experimental data mostly to the friction between particles and the PMMA plates which hold the samples in the out of plane direction. Although this was not modelled in the numerical simulations, there is still good quantitative agreement between all sets of results up to 13% compression where the MD results begins to deviate due to its aforementioned limitation. This affirms the robustness of the phenomena under investigation since each experimental arrangement will contain imperfections at different locations within the crystal. All of the curves are relatively smooth in accordance with the gradual and homogeneous transformation.

For larger size ratio χ , the transformation is inhomogeneous and proceeds through sudden local rearrangements of groups of particles. Snapshots of the experiment and finite element simulation

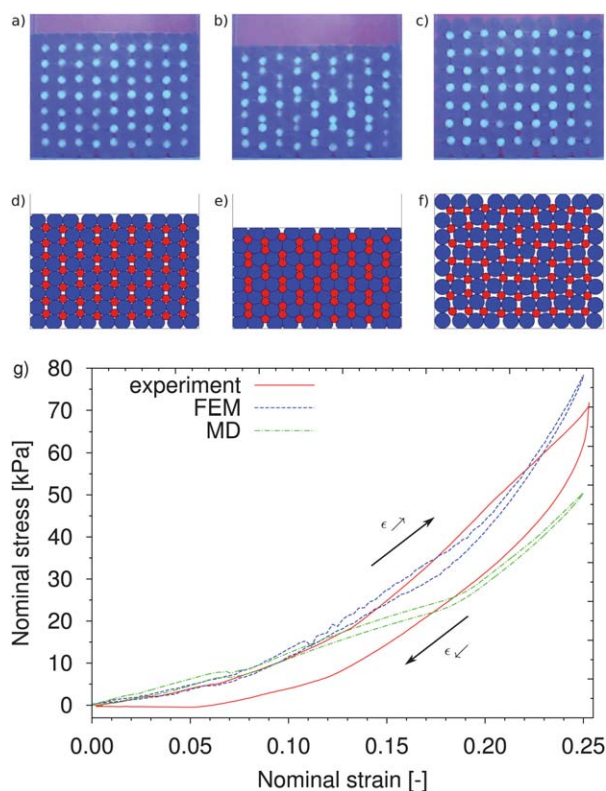


Fig. 2 Snapshots of the experiment (a, b, c) and Finite Element simulations (d, e, f) at 15%, 25% strain levels and after unloading for the crystal with size ratio $\chi = 0.53$. The transformation is homogeneous and occurring gradually over the loading phase. (g) Experimental and numerical stress–strain curves.

for the $\chi = 0.61$ crystal are shown in Fig. 3a–f. A rather disordered configuration is reached after unloading, hence the transformation is not reversible for this case. The jumps in the stress in Fig. 3g are associated with local rearrangements. In particular, the final state in the experiment is reached after a sudden stress drop at $\sim 16\%$ strain after the reordering of a diagonal structure which is reminiscent of a shear band.

The results of the experiments and the numerical simulations both indicate that the size ratio of the particles changes the qualitative nature of the pattern transformation process whereas the mechanical properties are of lesser importance. Indeed, we have performed FEM and MD simulations where the relative stiffness of the particles $E_{\text{small}}/E_{\text{large}}$ have been varied by three orders of magnitude and find that, for an appropriate size ratio, the characteristic pairing of small particles occurred irrespective of the relative particle stiffness. Moreover, we observe that large values of friction, loading rate or artificial damping can prevent pattern formation. However, small variations of these do not appear to change the qualitative nature of the pattern transformation.

Analytical calculations based on the structure of the crystal¹¹ before and after transformation and the assumption that both particle types are rigid can be used to provide an estimate of the range of size ratio where a paired pattern can occur. The minimum value $\chi_{\text{min}} = \sqrt{2} - 1$ is determined by the geometry of the initial square lattice such that large particles are touching and the small one in the middle is in contact with its neighbors. In practice, the pattern transformation is unlikely to occur in this situation because small

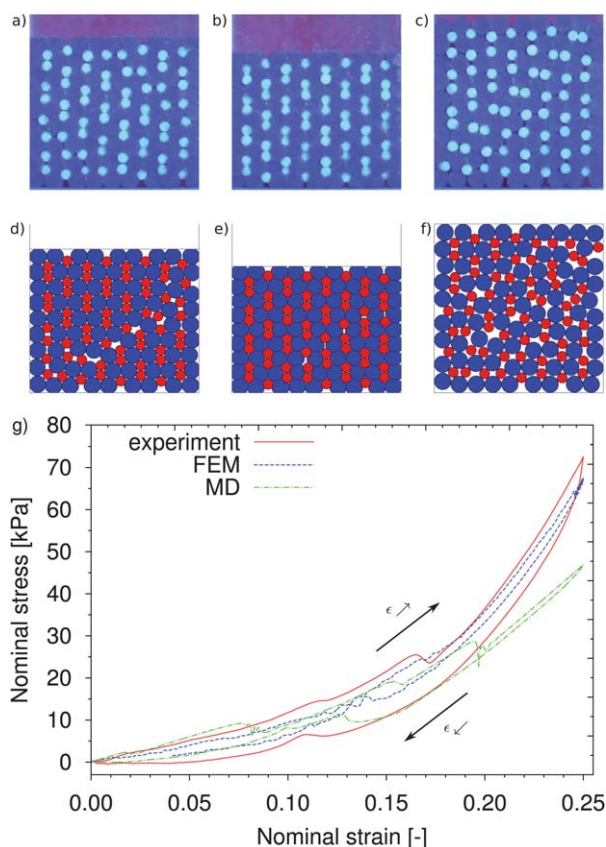


Fig. 3 Snapshots of the experiment (a, b, c) and Finite Element simulations (d, e, f) at 15%, 25% strain levels and after unloading for the crystal with size ratio $\chi = 0.61$. The transformation is inhomogeneous and happens as a result of a series of spontaneous local rearrangements. (g) Experimental and numerical plots of the stress-strain data. The drops in the stress correspond to reordering events.

particles are trapped inside the cage of large ones which strictly constrains their mobility. Similarly, the maximum size ratio $\chi_{\max} = 0.637$ is obtained when rigid particles satisfy the connectivity of the patterned state (see Fig. 1b, d).

To further investigate the qualitative difference induced by the size ratio, we have performed a series of simulations based on Energy Minimization (EM).¹² The total elastic energy of the system was computed by adding up the work of the contact forces. For the sake

of brevity, we present only the results for three cases which show a qualitatively distinct transformation behavior *i.e.* quasi-reversible ($\chi = 0.5$), irreversible ($\chi = 0.6$) and transformation leading to another non-periodic structure ($\chi = 1$). We monitored the structural changes of the crystals during loading using the concept of shape factor based on Voronoi tessellation of the particle centers introduced by Moucka and Nezbeda.¹³ The shape factor for a Voronoi cell associated with particle i is given by $\zeta_i = C_i^2/4\pi S_i$ where C_i and S_i are the cell's perimeter and surface area, respectively.

A contour plot of the probability distribution of the shape factors for the crystal with size ratio $\chi = 0.5$ over a cycle of loading and unloading is shown in Fig. 4a. Two distinct branches of high probability shape factors appear gradually as the packing is compressed and upon unloading the branches converge back. At maximum strain, the upper branch at $\zeta \approx 1.17$ corresponds to the Voronoi cells of the small (hard) particles which are irregular pentagons (at the patterned state). The lower branch which groups cells with shape factor $\zeta \approx 1.11$ corresponds to the Voronoi cells of the big (soft) particles which are heptagons (not regular; almost hexagons). The symmetry of the branches about 25% strain axis confirms the reversibility of the pattern transformation for this size ratio.

On the other hand, as can be seen in Fig. 4b, the evolution of the probability distribution of the shape factor ζ for the crystal with $\chi = 0.6$ is significantly different. First, two bands appear spontaneously around $\zeta \approx 1.16$ and $\zeta \approx 1.12$ at approximately 5% compression indicating that the characteristic structure of the pattern begins to form very early. Secondly, they remain until the end of the loading cycle. Thus, the transformation for $\chi = 0.6$ is irreversible in contrast with the crystal with size ratio $\chi = 0.5$ where reversibility was found. The evolution of the shape factor distribution for a crystal with size ratio $\chi = 1$ as function of compression is illustrated by the results shown in Fig. 4c. In this case the crystal develops a non-periodic structure and the deformation is irreversible.

In conclusion, a combined experimental and numerical study has been used to uncover a novel pattern transformation when regular arrays of macroscopic particles are subjected to uniaxial compression. The reversibility of the transition process only depends on the size ratio of the particles but the final transformed state is robust and it does not depend on the details of its evolution. The work was inspired by bifurcation sequences found in model martensitic transitions¹⁴ at the microscopic level. Connections can also be drawn with energy absorption processes at the macroscopic level in one-dimensional granular crystals which may be considered as shock absorbers and

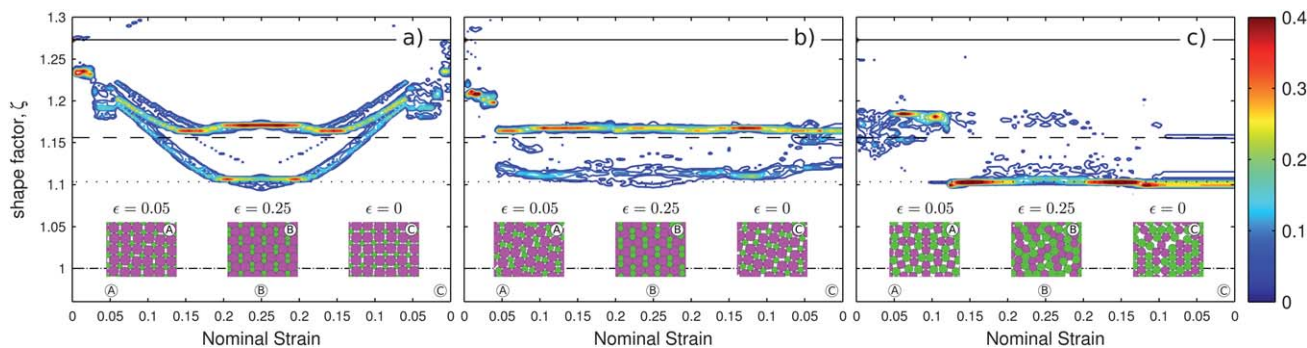


Fig. 4 Evolution of the probability distribution of the shape factor ζ in minimum energy configurations as function of compression for the size ratios (a) $\chi = 0.5$, (b) $\chi = 0.6$ and (c) $\chi = 1$. The solid, dashed, dotted and dashed-dotted lines denote the shape factors for squares $\zeta = 1.273$, regular pentagons $\zeta = 1.156$, regular hexagons $\zeta = 1.103$ and circles $\zeta = 1$, respectively.

nonlinear acoustic lenses.^{15–17} We believe that the 2D granular crystals studied in the current study combined with pattern transformation can find equivalently interesting applications as tunable phononic devices.^{3,4} Furthermore, we expect that the same mechanism will persist at microscopic scales leading to exciting prospects such as color tuning by mechanical loading¹⁸ and novel applications in photonic crystals.^{5,19}

Acknowledgements

SW and TM acknowledge the support of João Fonseca and Stuart Morse of the school of Materials in Manchester University. FG and SL acknowledge financial support from the Delft Center for Computational Science and Engineering and the Institute of Mechanics Processes and Control Twente. KB and JS acknowledge financial support from Harvard University.

Notes and references

† Contact force parameters used in MD simulations for the crystal with size ratio $\chi = 0.51$: *Soft–Soft* $k_1 = 1.3458 \text{ N mm}^{-1}$, $k_2 = 0.1264 \text{ Nmm}^{-\alpha}$ and $\alpha = 2.9792$, *Soft–Hard* $k_1 = 2.6443 \text{ N mm}^{-1}$, $k_2 = 0.1816 \text{ N mm}^{-\alpha}$ and $\alpha = 3.4942$, *Hard–Hard* $k_1 = 3362.8 \text{ N mm}^{-1}$, $k_2 = 1597.2 \text{ N mm}^{-\alpha}$ and $\alpha = 2.7198$ and for the crystal with size ratio $\chi = 0.61$: *Soft–Hard* $k_1 = 2.8328 \text{ N mm}^{-1}$, $k_2 = 0.1274 \text{ N mm}^{-\alpha}$ and $\alpha = 3.7673$, *Hard–Hard* $k_1 = 3205.5 \text{ N mm}^{-1}$, $k_2 = 1393.7 \text{ N mm}^{-\alpha}$ and $\alpha = 2.5769$.

- 1 S. Singamaneni and V. V. Tsukruk, *Soft Matter*, 2010, **6**, 5681–5692.
- 2 T. Mullin, S. Deschanel, K. Bertoldi and M. C. Boyce, *Phys. Rev. Lett.*, 2007, **99**, 084301.
- 3 K. Bertoldi and M. C. Boyce, *Phys. Rev. B: Condens. Matter Mater. Phys.*, 2008, **77**, 052105.
- 4 J. H. Jang, C. Y. Koh, K. Bertoldi, M. C. Boyce and E. L. Thomas, *Nano Lett.*, 2009, **9**, 2113–2119.
- 5 X. Zhu, Y. Zhang, D. Chandra, S.-C. Cheng, K. J. M and S. Yang, *Appl. Phys. Lett.*, 2008, **93**, 161911.
- 6 B. A. Grzybowski, A. Winkleman, J. A. Wiles, Y. Brumer and G. M. Whitesides, *Nat. Mater.*, 2003, **2**, 241–245.
- 7 S. Koh, *Nanoscale Res. Lett.*, 2007, **2**, 519–545.
- 8 L. R. G. Treloar, *Trans. Faraday Soc.*, 1943, **39**, 241–246.
- 9 S. Luding, *Granular Matter*, 2008, **10**, 235–246.
- 10 M. Lundberg, K. Krishan, N. Xu, C. S. O'Hern and M. Dennin, *Phys. Rev. E: Stat., Nonlinear, Soft Matter Phys.*, 2008, **77**, 041505.
- 11 C. N. Likos and C. L. Henley, *Philos. Mag. B*, 1993, **68**, 85–113.
- 12 C. S. O'Hern, L. E. Silbert, A. J. Liu and S. R. Nagel, *Phys. Rev. E: Stat., Nonlinear, Soft Matter Phys.*, 2003, **68**, 011306.
- 13 F. Moucka and I. Nezbeda, *Phys. Rev. Lett.*, 2005, **94**, 040601.
- 14 R. S. Elliott, N. Triantafyllidis and J. A. Shaw, *J. Mech. Phys. Solids*, 2006, **54**, 161–192.
- 15 E. B. Herbold, J. Kim, V. F. Nesterenko, S. Wang and C. Daraio, *Acta Mech.*, 2009, **205**, 85–103.
- 16 C. Daraio, E. B. Nesterenko, V. F. Herbold and S. Jin, *Phys. Rev. Lett.*, 2006, **96**, 058002.
- 17 A. Spadoni and C. Daraio, *Proc. Natl. Acad. Sci. U. S. A.*, 2010, **107**, 7230–7234.
- 18 K. Jeong, J. Jang, C. Koh, M. Graham, K. Jin, S. Park, C. Nah, M. Lee, S. Cheng and E. Thomas, *J. Mater. Chem.*, 2009, **19**, 1956–1959.
- 19 J. Yang, C. Schreck, H. Noh, S. Liew, M. I. Guy, C. S. O'Hern and H. Cao, *Phys. Rev. A: At., Mol., Opt. Phys.*, 2010, **82**, 053838.